

# Modelling the TeV $\gamma$ -ray spectra of two low redshift AGNs: Mkn 501 & Mkn 421

A. Konopelko

*Max-Planck-Institut für Kernphysik, Postfach 10 39 80, Heidelberg, Germany*

A. Mastichiadis

*Department of Physics, University of Athens, Panepistimiopolis, GR 15783, Zografos,  
Greece*

J. Kirk

*Max-Planck-Institut für Kernphysik, Postfach 10 39 80, Heidelberg, Germany*

O.C. de Jager

*Unit for Space Physics, Potchefstroom University, 2520, South Africa*

F.W. Stecker

*Laboratory of High Energy Astrophysics, NASA Goddard Space Flight Center, Greenbelt,  
MD 20771, USA*

## ABSTRACT

We discuss the results of modelling the TeV  $\gamma$ -ray spectra of two AGNs, Mkn 501 and Mkn 421 that have almost the same redshifts:  $z = 0.031$  and  $z = 0.034$ , respectively. The effect of intergalactic  $\gamma$ -ray absorption is treated as an uncertainty in the measurement of the intrinsic spectrum. Although the objects differ, we obtain satisfactory fits for both of them in a synchrotron self-Compton scenario. Compared to previous models, our fits are characterised by higher values of the Doppler factor ( $\delta \geq 50$ ) and an electron injection spectrum extending to higher energies ( $\gamma_{\max} \geq 1.5 \times 10^5$ ). In the case of Mkn 421, the observed difference in spectral slope in X-rays and TeV  $\gamma$ -rays between the high and low states can be explained as a variation of a single parameter — the maximum energy  $\gamma_{\max} mc^2$  at which electrons are injected.

*Subject headings:* SSC models of blazars

## 1. Introduction

Ground-based detectors, utilizing the imaging atmospheric Čerenkov technique, provide an effective tool for the study of cosmic TeV  $\gamma$ -rays. Recently, several celestial objects have been identified as TeV  $\gamma$ -ray emitters using this technique (Ong 1998; Catanese & Weekes 1999). Among these are a few active galactic nuclei located at different redshifts: Mkn 421 ( $z = 0.031$ ) (Punch et al. 1992), Mkn 501 ( $z = 0.034$ ) (Quinn et al. 1996), 1ES 2344+514 ( $z = 0.44$ ) (Catanese et al. 1998), 1ES 1959+650 ( $z = 0.048$ ) (Nishiyama et al. 2000), PKS 2155-304 ( $z = 0.117$ ) (Chadwick et al. 1999) and 1ES 1426+428 ( $z = 0.129$ ) (Horan et al. 2002).

Several explanations have been advanced for the formation of the spectrum of these objects, starting from an injection of energy in the form of either energetic hadrons (Mannheim & Biermann 1992; Mannheim 1993, 1998; Mücke & Protheroe 2001; Aharonian 2000) or energetic electrons (e.g., Maraschi, Ghisellini & Celotti (1992); Marscher & Travis (1996); Inoue & Takahara (1996); Kino, Takahara & Kusunose (2002)). At present it is not possible to eliminate either of these possibilities on the basis of observation. However, the most widely investigated model involves the injection of relativistic electrons and the production of TeV photons via the synchrotron self-Compton (SSC) mechanism and in this paper we adhere to this scenario.

Some forty years ago it was suggested that TeV  $\gamma$ -rays could be absorbed by interacting with diffuse interstellar or intergalactic infra-red (IR) radiation (Nikishov 1962; Gould & Schreder 1966). Following the discovery by the *EGRET* team that the blazar 3C279 at a redshift of 0.54 was an emitter of a powerful flux of high energy  $\gamma$ -rays (Hartman et al. 1992), it was suggested by Stecker, de Jager & Salamon (1992) that such powerful extragalactic sources would be useful as probes of the extragalactic infrared radiation because of the absorption caused by pair-production interactions of their TeV  $\gamma$ -rays. Stecker, de Jager & Salamon (1992) further derived the formula for the redshift dependence of this absorption and showed that the absorption coefficient would be highly dependent on redshift.

Owing to the lack of direct measurements of the IR background radiation in the wavelength range 1–50  $\mu\text{m}$  (Hauser & Dwek 2001), a computation of the opacity of the intergalactic medium to TeV  $\gamma$ -rays must be based on a model of the diffuse radiation field. The lower limits on the extra-galactic background light (EBL) at 7  $\mu\text{m}$  and 15  $\mu\text{m}$  set by ISO-CAM measurements (Franceschini et al. 2001) have ruled out a number of such models that underestimate the EBL distribution and have significantly constrained others. Improved computations of the intergalactic opacity reveal, in turn, new information on the intrinsic TeV spectra of AGN. In this paper we apply the SSC model to the two best observed TeV sources, using opacities computed from models of the EBL that satisfy the most recent

constraints.

In principle, one can attempt to predict directly the TeV measurements, by combining a theoretical model of intrinsic spectrum of the AGN with one of the intergalactic absorption. This would enable an unambiguous comparison of prediction with observation and, via a maximum likelihood approach, an estimate of the “best-fit” parameters. However, the absorption model is subject to observational constraints independent of the TeV measurements. These constraints allow a range of possibilities, each of which can be associated with a different likelihood of realisation. In order to take this into account, it would be necessary to assign a range of values to each predicted flux point, confusing the procedure of maximising the overall likelihood.

In this paper, we adopt a different approach, similar to that used in Konopelko et al. (1999). There, it was shown that for the EBL distribution given by Malkan & Stecker (1998) the homogeneous SSC model provides a reasonable fit to the intrinsic TeV  $\gamma$ -ray spectrum of Mkn 501. Here, we use the revised distributions of the EBL given by Malkan & Stecker (2001) to estimate both the magnitude and the uncertainty in the absorption and construct intrinsic spectra using several sets of TeV data, before fitting them with a homogeneous SSC model. In particular, we use the results recently obtained by the Whipple (Krennrich et al. 2001) and HEGRA (Aharonian et al. 2002) groups on Mkn 421 during its flaring state in 2001, which provide statistics unprecedented in TeV astronomy, with more than 30,000 photons detected.

Previous discussions of the intrinsic spectrum of TeV blazars have used specific forms for the absorption optical depth, rather than estimating an uncertainty. Thus, Konopelko et al. (1999) obtained the intrinsic spectrum of Mkn 501 using the combined spectrum of the Whipple and HEGRA groups and applying the optical depth,  $\tau = \tau(E_\gamma, z)$ , calculated by de Jager & Stecker (1998) based on the predictions on SED of intergalactic IR photon field from Malkan & Stecker (1998). The unfolded spectrum was close to a power-law of index 2.0 within the energy range starting from 500 GeV and extending up to 20 TeV. Using a similar method for the optical depth derived from simplified calculations of the SED of EBL over optical, IR and far-IR wavelengths, Kneiske, Mannheim & Hartmann (2002) obtained an intrinsic spectrum of Mkn 501, which is consistent with a power-law of 2.49. Using another similar method, de Jager & Stecker (2002) reconstructed the intrinsic spectrum of Mkn 501 as a power-law of index  $\sim 1.6$ – $1.7$  up to  $\sim 5$ – $10$  TeV. Protheroe & Meyer (2000) had previously obtained an upturn in the intrinsic spectrum in this energy range. However, such an upturn does not occur when the recalibrated HEGRA data for Mkn 501 (Aharonian et al. 2001) and a more realistic SED of the EBL is used, in which the  $60 \mu\text{m}$  flux reported by Finkbeiner, Davis & Schlegel (2000) is not taken into account. Aharonian et al. (2002a)

have also derived the intrinsic spectrum of Mkn 501 for a specific SED of EBL which also excludes the controversial  $60\ \mu\text{m}$  data point.

Having constructed the intrinsic spectrum we use the SSC model described by Maticchiadis & Kirk (1997) to obtain a fit. Several groups have recently published fits to both the X-ray and TeV  $\gamma$ -ray spectra of Mkn 421 and Mkn 501 (see e.g., Tavecchio et al. (2001); Krawczynski et al. (2001); Kino, Takahara & Kusunose (2002)) using schemes similar to this one. However in these papers, the effect of intergalactic IR  $\gamma$ -ray absorption was not emphasized. Here we test the SSC model against the *de-absorbed* TeV  $\gamma$ -ray spectra of two BL Lac's, Mkn 421 and Mkn 501. The IR absorption of multi-TeV  $\gamma$ -rays substantially changes the intrinsic source spectra and strongly influences the optimum values of the model parameters we find. In particular, taking account of extragalactic absorption moves the peak of the intrinsic spectrum to higher energies. Thus, Tavecchio, Maraschi & Ghisellini (1998), by not taking account of absorption, placed the Compton peak in the Mkn 501 in the sub-TeV range and could not generate a logically consistent SSC model, whereas de Jager & Stecker (2002), taking account of absorption, showed that the peak in the intrinsic spectrum of Mkn 501 was  $\sim 8$  TeV.

The BL Lac objects Mkn 501 and Mkn 421 have similar redshifts ( $z = 0.031$  and  $z = 0.034$ , respectively) so that the effects of intergalactic absorption are almost identical. Observations of both of these objects show a softening of the spectrum to higher energies. However, the intrinsic, *de-absorbed* spectra, are very different, while the two objects have rather different variability patterns. Nevertheless, the SSC model provides a reasonable fit to both of them, indicating large Doppler factors ( $\delta > 50$ ) and high, but different, values for the maximum energy at which electrons are injected. Thus, the exponential cut-offs found at similar energies in observations of both sources should be interpreted as due to the effect of intergalactic absorption and not taken as evidence of similarities in the physical conditions intrinsic to the two sources. Recent data for other AGNs detected at larger redshifts — 1ES1426+428 ( $z = 0.129$ ) and PKS 2155-304 ( $z = 0.117$ ), are consistent with this interpretation.

## 2. Observations

Since their discovery in TeV  $\gamma$ -rays two BL Lac objects Mkn 501 and Mkn 421 have been continuously monitored by a number of ground-based imaging atmospheric Čerenkov telescopes, e.g., CAT (Barrau et al. 1998), HEGRA (Konopelko et al. 1999a), Whipple (Finley et al. 2001). Even though the calibration of a Čerenkov telescope is not an easy procedure, it can ultimately be tested by joint measurements of the energy spectrum of a

source selected as a standard. Recent measurements of the TeV energy spectrum of the Crab Nebula performed by these groups are consistent within the quoted statistical errors (see Aharonian et al. (2000)). Thus spectral measurements performed on any particular source by different groups can be considered as complementary. In this section we briefly review the results of observations of several TeV-emitting BL Lac objects in X-rays and  $\gamma$ -rays.

### 2.1. Mkn 501

The BL Lac object Mkn 501 was first detected by the Whipple group (Quinn et al. 1996) in TeV  $\gamma$ -rays and was later confirmed by the HEGRA group (Bradbury et al. 1997). Early detections of Mkn 501 revealed a very low flux of TeV  $\gamma$ -rays, at the level of about 0.5 Crab (1 Crab corresponds to the constant flux from the Crab Nebula). However, in 1997 Mkn 501 exhibited an unprecedented flare in TeV  $\gamma$ -rays with an integral flux of up to 10 Crab. A very long exposure on this source, lasting almost 6 months, yielded unprecedented statistics for TeV  $\gamma$ -rays, which provided very accurate measurements of the spectrum (Samuelson et al. 1998; Krennrich et al. 1999; Aharonian et al. 1999, 2001; Djannati-Atai et al. 1999) over the energy range from 250 GeV up to 20 TeV. The spectrum of Mkn 501 is evidently curved and can be empirically fit by a power-law with an exponential cut-off at energy  $E_0$ :  $(dN_\gamma/dE) \propto E^{-\alpha} \exp(-E/E_0)$ . For such a spectrum, showing a gradual steepening of the spectral slope, one can expect a significant spill-over of the low energy events towards the higher energies, given a limited energy resolution. However, even for the rather modest energy resolution of the 10 m Whipple telescope — which is about 30% (Mohanty et al. 1998) — the effect of spill-over may not be very important, because the energy spectrum below 10 TeV is relatively flat. The HEGRA system of IACTs has noticeably better energy resolution (about 10–20%, see Hofmann et al. (2000)). Recent studies show that the effect of spillover for HEGRA data is almost negligible up 17 TeV and has a limited effect above that energy (Aharonian et al. 1999).

In the energy range between 0.5 and 10 TeV, the Whipple Mkn 501 data are in good agreement with the HEGRA Mkn 501 data. Hereafter, we use in our analysis the combined energy spectrum of Mkn 501 as measured by both groups, which extends from 260 GeV up to 22 TeV. Note that the analysis of the HEGRA Mkn 501 data taken during the flaring state in 1997 has shown that the shape of the energy spectrum does not depend on the flux level (Aharonian et al. 1999). This was confirmed by analysis of the Whipple Mkn 501 data taken during the same observational period (Samuelson et al. 1998; Krennrich et al. 1999). Despite some evidence of spectral variations in Mkn 501 reported by Djannati-

Atai et al. (1999) and Aharonian et al. (2001a) for specific observational periods, such spectral variation cannot be considered as an established feature of the source. Additional observations of Mkn 501 are needed in order to prove or disprove this point. In addition, there are no contemporaneous X-ray data available for those observational periods which show a slight deviation of the TeV  $\gamma$ -ray spectra from its time-averaged spectral shape. Thus we do not discuss here the possible scenario of the simultaneous X-ray and TeV  $\gamma$ -ray flare for Mkn 501, even though the main conclusions, regarding the environmental parameters of the TeV  $\gamma$ -ray emission should certainly apply to any state of Mkn 501. For the additional fine tuning of the model parameters one needs more simultaneous multi-wavelength observations of this source.

Mkn 501 is a highly variable source of TeV  $\gamma$ -ray emission. The shortest variability discovered has a doubling time of  $\sim 20$  mins (Sambruna et al. 2000). Such fast variability of the source is associated with sporadic changes of the flux level on much longer time scales. The source can be in a flaring state ( $\geq 3$  Crab) as well as in a very low state ( $\sim 0.1$  Crab) for a few months.

Occasionally Mkn 501 shows a very strong flux of X-ray emission (see (Tavecchio et al. 2001)). For example, during the 1997 flare the BeppoSAX satellite detected a dramatic increase in the X-ray flux up to 100 keV (Pian et al. 1997) with a very flat spectral slope. Simultaneous multi-wavelength observations of Mkn 501 revealed clear correlations between the X-ray and the TeV  $\gamma$ -ray fluxes (Catanese et al. 1997; Petry et al. 2000; Sambruna et al. 2000), even though the rapid X-ray flares from Mkn 501 are not always accompanied by a high emission state in TeV  $\gamma$ -rays (Catanese & Sambruna 2000).

We used here the data taken with *BeppoSAX* in observation period of April 1997 as discussed in detail by (Pian et al. 1997). These data were combined with the time-averaged TeV  $\gamma$ -ray spectrum as measured by HEGRA in 1997 observational campaign (Aharonian et al. 1999).

## 2.2. Mkn 421

The BL Lac object Mkn 421 is one of the AGNs detected by the EGRET instrument on board Compton GRO in the 30 MeV–30 GeV energy range (Thompson et al. 1995). It was the first extra-galactic TeV  $\gamma$ -ray source, discovered by the Whipple group (Punch et al. 1992) and was confirmed by the HEGRA group (Petry et al. 1996). Since its discovery, Mkn 421 has shown a very low baseline TeV  $\gamma$ -ray emission with a few extremely rapid flares on timescales from one day to 30 minutes (Gaidos et al. 1996). The limited statistics

of the  $\gamma$ -ray events recorded during the short duration flares, as well as the long exposure observations during the very low emission state, did not permit a measurement of the energy spectrum above 7 TeV (Krennrich et al. 1999; Aharonian et al. 1999a). Only recently, in 2000 and 2001, has Mkn 421 demonstrated a flare with an average flux of 4 Crab

(Krennrich et al. 2001; Aharonian et al. 2002; Krennrich et al. 2002). Data taken during this flare have been used to extract the energy spectrum of Mkn 421 at higher energies, up to 20 TeV. As stated by both groups, the energy spectrum of Mkn 421 is evidently curved. Analysis of the HEGRA Mkn 421 data revealed significant variations of the spectral slope at energies below 3 TeV (Aharonian et al. 2002; Krennrich et al. 2002), with the high flux state showing a substantially harder spectrum. However the best empirical fit to the data taken in both the high and the low states gives the same cut-off energy of 3.6 TeV. This is consistent with the assumption that all spectra are affected by intergalactic absorption. The cut-off energy derived from the Whipple data on Mkn 421 (Krennrich et al. 2001, 2002) is 4 TeV. Given the statistical and systematic errors of such a measurement this value agrees with that measured by HEGRA group (Aharonian et al. 2002).

Mkn 421 is a bright, variable X-ray source. Its X-ray energy spectrum was measured in different states of emission by the BeppoSAX instrument (Fossati et al. 2000) within the range from 0.1 keV up to 10 keV and the RXTE instrument up to 100 keV. During the flares, the peak of the X-ray emission moves towards high energies (Fossati et al. 2000). Note that the peak position in the X-ray spectrum of Mkn 421 is substantially lower ( $\sim 1$  keV) than the peak in the X-ray spectrum of Mkn 501 ( $\sim 100$  keV) in its flaring state. This implies intrinsic physical differences between the two sources.

We used here the fits of the X-ray spectra of Mkn 421 measured with the *BeppoSAX* in 2000 for low and high states of the source (Fossati et al. 2002) (see Figure 5). These data were combined with the two time averaged HEGRA spectra (Aharonian et al. 2002) of Mkn 421 derived from the data taken mostly in 2000 (see Figure 2 in (Aharonian et al. 2002)) for two observational periods when Mkn 421 was in high and low states.

### 2.3. 1ES 1426+428

1ES 1426+428 is a BL Lacertae object (see (Remillard et al. 1989)) at a redshift of  $z = 0.129$ . Recent BeppoSAX observations (Costamante et al. 2001) revealed for this source a rather flat ( $\alpha = 0.92$ ) power-law X-ray spectrum extending up to 100 keV, without evidence for a spectral break. Such extreme behavior of the source in X-rays is reminiscent of the BL Lacertae object Mkn 501 previously detected at TeV energies. Estimates of the

TeV  $\gamma$ -ray flux from 1ES 1426+428 obtained in a homogeneous synchrotron self-Compton (SSC) model (Costamante et al. 2001) suggested that this source should be detectable at TeV energies.

This was confirmed by the detection of 1ES 1426+428 recently reported by the Whipple group (Horan et al. 2002). The source was also detected by the HEGRA group (Aharonian et al. 2002b) during the same observational period in 2000 and 2001. HEGRA also measured the energy spectrum of 1ES 1426+428 (Aharonian et al. 2002b). Recent spectral measurements made by Whipple (Petry et al. 2002) and CAT (Djannati-Atai et al. 2002) generally confirmed HEGRA spectrum of 1ES 1426+428. The limited statistics of the detected  $\gamma$ -rays does not allow a study of flux and spectral variability. A preliminary estimate of the spectral shape is consistent with a rather steep power-law spectrum and a significant  $\gamma$ -ray rate above 3 TeV (Aharonian et al. 2002b). Note that 1ES 1426+428 has a redshift substantially larger than the two well-established BL Lac objects, Mkn 421 and Mkn 501. Therefore, IR absorption should significantly modulate the intrinsic TeV  $\gamma$ -ray spectrum of this object. However, current 1ES 1426+428 data are rather limited in statistics and cannot be used to place stringent constraints on the distribution of EBL.

#### 2.4. Other TeV BL Lacs

For the three remaining AGN detected at TeV energies, namely 1ES 2344+514 (Catanese et al. 1998), 1ES 1959+650 (Nishiyama et al. 2000), and PKS 2155-304 (Chadwick et al. 1999), there are still no data available on the spectral shape. 1ES 1959+650 was detected recently by Whipple (Weekes et al. 2002) and HEGRA (Horns & Konopelko 2002) in a very high state ( $\geq 3$  Crab), but the spectral measurements have not yet been published. The TeV  $\gamma$ -ray fluxes reported for 1ES 2344+514, 1ES 1959+650, and PKS 2155-304, are consistent with the IR absorption model used here. These data do not constrain the model severely because of the rather large uncertainties of the measured TeV  $\gamma$ -ray spectra.



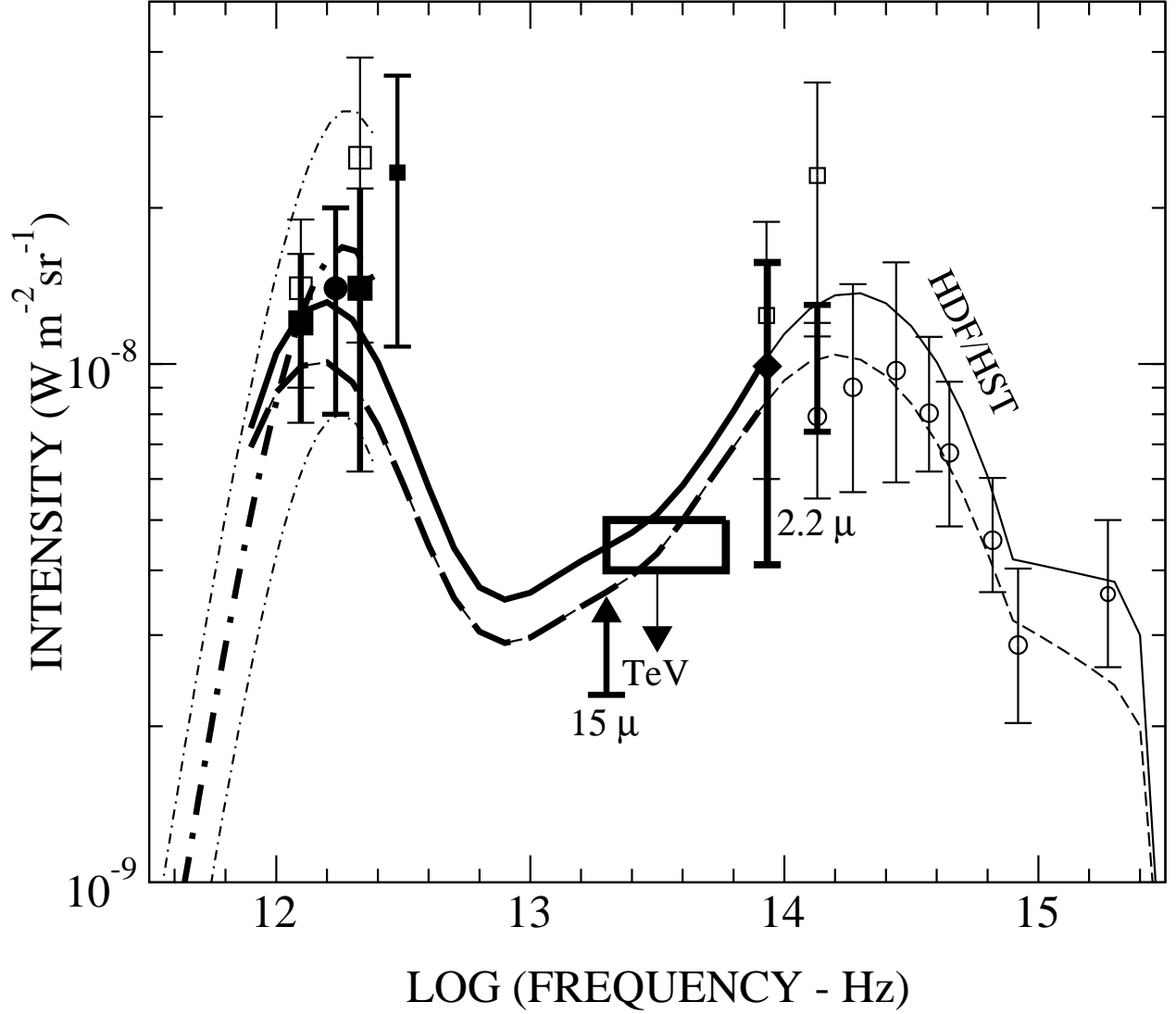


Fig. 1.— The SED of the EBL. Solid and dashed curves correspond to the Malkan & Stecker (2001) data obtained assuming the *rapid* as well as *baseline* luminosity evolutionary model, respectively. The infrared luminosities of galaxies is assumed to increase as  $(1+z)^3$  from  $z_1 = 0$  back to  $z_2 = 2$  for the lower curve, and as  $(1+z)^4$  from  $z = 0$  back to  $z_2 = 1.4$  for the upper curve. Both curves have been derived assuming a flat star formation rate at  $z > z_2$ .

### 3. Opacity of TeV $\gamma$ -rays

TeV  $\gamma$ -rays can be absorbed and produce electron-positron pairs on interaction with photons of the intergalactic background light (see Stecker, de Jager & Salamon (1992)). The corresponding opacity can be calculated once an assumption is made about the spectral energy distribution (SED) of the extra-galactic background light (EBL).  $\gamma$ -rays of energy from 300 GeV to 20 TeV interact most effectively with photons of wavelength from 1–50  $\mu\text{m}$ , respectively. There have been a number of attempts in past to measure the SED of EBL in this range as well as to model it (for a review see Hauser & Dwek (2001)). Recently Malkan & Stecker (2001) revised their empirically based model (Malkan & Stecker 1998) for the EBL starting from the near-IR and extending to the far-IR range (see Fig. 1). This model is consistent with all currently measured lower and upper limits in the mid-IR range as well as with the COBE-FIRAS fluxes given at 140  $\mu\text{m}$  and 240  $\mu\text{m}$ . In addition, de Jager & Stecker (2002) extended the EBL derived in (Malkan & Stecker 2001) to ultraviolet (UV) wavelengths using the galaxy counts in the Hubble Deep Field data taken with Hubble Space Telescope (see Madau & Pozzetti (2000)). The so-called *hybrid* model developed by de Jager & Stecker (2002) gives a smooth distribution of the EBL over the 1–300  $\mu\text{m}$  wavelength range. It is consistent with existing measurements and upper limits in the optical–UV range and agrees rather well with similar theoretical models (e.g. Tan, Silk & Balland (1999); Rowan-Robinson (2001); Xu (2000)) in the mid-IR range. Note that all of those models predict a flat distribution of EBL in the mid-IR range at a flux level of about 3–4  $\text{nW m}^{-2}\text{sr}^{-1}$ . However, direct measurements of the EBL in the mid-IR range are hampered by unavoidable foreground emission (for a detailed discussion see Hauser & Dwek (2001)).

An alternative approach to finding the SED of EBL in the relevant energy range is provided by semi-analytical modelling of the evolution of galaxy formation (see Primack (2002)). However, the results of this approach are sensitive, for example, to the IMF assumed in the calculations. In fact different IMFs result in rather different SEDs (see Primack (2002) and references therein). Specific sets of model parameters succeed rather well in reproducing the phenomenological hybrid model developed by Malkan & Stecker (2001), and such models could in principle be used in conjunction with an SSC model of the intrinsic emission of an AGN to predict the TeV flux. However, in this paper it is not our goal to test both the SSC and the absorption models simultaneously. Instead, we wish to test only the SSC model and include the uncertainties in the level of absorption into an additional error to be added to that already present in the TeV observation. To this end, we consider the two extreme cases of high and low flux SEDs as given by Malkan & Stecker (2001) as shown in Fig. 1. One can see that in the mid-IR region the upper limits derived from the TeV  $\gamma$ -ray data (see e.g. Renault et al. (2001)) and the low limits established from the data taken by ISOCAM instrument (see Franceschini et al. (2001)) are very close to each other. They

stringently limit the allowed region for the actual SED of EBL in this range. For the extreme cases considered by Malkan & Stecker (2001), de Jager & Stecker (2002) have calculated the optical depth,  $\tau(E_\gamma, z)$ , of the  $\gamma$ -rays of energy  $E > 50$  GeV for redshifts up to  $z = 0.3$ . Using the parametric expression given in Eq. (1,2) in de Jager & Stecker (2002), we interpret the resulting upper and lower values of the “de-absorbed” intrinsic flux

$$(dN_\gamma/dE)_{\text{intrinsic}} = (dN_\gamma/dE)_{\text{measured}} \cdot \exp[\tau(E, z)]. \quad (1)$$

as  $3\sigma$  deviations from the true value, and add this error to that attached to the original TeV point.

The resulting intrinsic spectra for both the flaring and quiescent states of Mkn 501 and for Mkn 421 shown in Figure 2,3. All of these spectra show a prominent peak in the  $E^2F(E)$  distribution. The position of the peak is at about 8 TeV and 2 TeV for Mkn 501 and Mkn 421, respectively. These objects have significantly different X-ray spectra, which are shown in Figs. 4 and 5, respectively.

#### 4. Modelling

To model the multi-wavelength spectra of the BL Lac objects Mkn 421 and Mkn 501 in a homogeneous SSC scenario we use an approach described by Mastichiadis & Kirk (1995, 1997). This method involves prescribing an injection function for relativistic electrons and solving the two time-dependent kinetic equations for the electron and photon distributions source. All relevant physical processes are taken into account in the code, i.e., synchrotron radiation, inverse Compton scattering (both in the Thomson and Klein-Nishina regimes), photon-photon pair production, and synchrotron self-absorption. Both synchrotron and inverse Compton scattering emissivities have been improved from the original version (Mastichiadis & Kirk 1995) and now incorporate the full emissivity rather than a delta-function approximation.

Seven model parameters are required to specify a source in a stationary state. These are:

1. the Doppler factor  $\delta = 1/[\Gamma(1 - \beta \cos \theta)]$ , where  $\Gamma$  and  $c\beta$  are the Lorentz factor and speed of the source, and  $\theta$  is the angle between its direction of motion and the line of sight to the observer,
2. the radius  $R$  of the source (in its rest frame, in which it is assumed spherical) or, equivalently, the crossing time  $t_{\text{cr}} = R/c$ . This is related to the observed minimum variation timescale in the galaxy frame by  $t_{\text{var}} = R/(\delta c)$ ,

3. the magnetic field strength  $B$ ,
4. the index  $s$  of the electron injection spectrum, for which we take  $Q_e = q_e \gamma^{-s} e^{-\gamma/\gamma_{\max}}$  where  $\gamma$  is the electron Lorentz factor,
5.  $\gamma_{\max}$ , the Lorentz factor at the cut-off of the injection spectrum
6.  $q_e$ , the amplitude of the injection spectrum, which is expressed in terms of the electron injection compactness  $\ell_e = \frac{1}{3} m_e c \sigma_T R^2 \int_1^\infty d\gamma (\gamma - 1) Q_e$  (Mastichiadis & Kirk 1995),
7.  $t_{\text{esc}}$ , the effective escape time of relativistic electrons, which can be identified as the timescale over which adiabatic expansion losses limit the accumulation of relativistic electrons within the source.

It is possible to introduce a lower limit to the Lorentz factor at which electrons are injected (Krawczynski, Coppi & Aharonian 2002). This permits more flexibility in fitting the soft X-ray spectrum and leads to different values of the parameter  $s$ , which is then no longer related to the low frequency spectral index. However, at TeV  $\gamma$ -ray energies, the models are essentially identical.

In attempting to optimize a fit to a particular data set, it is essential to use a physically motivated strategy to arrive at reasonable starting values for these seven parameters. This is done by identifying six scalars which characterise the typical blazar spectrum:

1. the peak frequency  $\nu_{s,18}$  of the synchrotron emission expressed in units of  $10^{18}\text{Hz}$
2. the peak frequency  $\nu_{c,27}$  of the inverse Compton emission, expressed in units of  $10^{27}\text{Hz}$
3. the total nonthermal luminosity  $L$
4. The approximate ratio  $\eta$  of the total flux in the inverse Compton part to that in the synchrotron part of the spectrum
5. the break frequency  $\nu_{\text{bf}}$  in the synchrotron part (typically between millimeter and optical wavelengths) of the spectrum, where cooling and electron escape or expansion losses are comparable
6. the low-frequency spectral index

Together with an estimate of the fastest variability timescale  $t_{\text{var}}$ , these roughly estimated quantities or *observables* enable one to find reasonable starting values of the seven parameters of the SSC model. However, this method works only if the intrinsic spectrum is

available. In particular, it is not possible to estimate quantities  $\nu_{c,27}$  (2) or  $\eta$  (4) unless the observed spectrum has been unfolded using an absorption model.

Following (Mastichiadis & Kirk 1997) we can find an estimate of the Doppler factor in terms of the observables:

$$\delta = 55 \nu_{c,27}^{1/2} t_3^{-1/4} \nu_{s,18}^{-1/4} L_{46}^{1/8} \eta^{-1/8} \quad (2)$$

where  $L_{46}$  is the nonthermal luminosity in units of  $10^{46}$  erg/s and  $t_3$  is the variation timescale in units of  $10^3$ s. From this follow the radius, magnetic field and Lorentz factor at the cut-off:

$$R = ct_{\text{var}}\delta; \quad B = 5 \times 10^{-3} \delta \nu_{s,18} \nu_{c,27}^{-2} \text{G}; \quad \gamma_{\text{max}} = 3 \times 10^6 \nu_{c,27} \delta^{-1} \quad (3)$$

The power-law index  $s$  is limited by radio data of Mkn 421 and Mkn 501 to be close to 1.5–1.7 provided, as we assume here, that the radiowaves are created in the same region as the high energy photons. In this case, the parameter  $\gamma_{\text{max}}$  is important, since most of the power is injected at the highest permitted values of the Lorentz factor. The remaining parameters are the electron compactness  $\ell_e$ , and the escape time  $t_{\text{esc}}$  which do not have a strong influence on the shape of the X-ray and TeV spectra, but only on the flux levels.

Using these starting values, we find the best fit models for the high and low states of Mkn 421 and Mkn 501 as given in Table 1. In each case, the differences between the optimal parameter values and the starting values given by Eq. (2) and (3) are small. The  $\chi^2$  values associated with these fits, taking into account the error introduced by the uncertainty in intergalactic absorption are unusually small. This indicates two things: 1) the SSC model provides a good fit and 2) the errors inferred from uncertainty in SED of IR are probably too generous. We may conclude that the actual value of the intergalactic absorption lies closer to the mean of the two extreme models given by Malkan & Stecker (2001) than suggested by our assumption that these represent  $1\sigma$  deviations.

In Figure 2 and 3 we show the fits for both BL Lac objects, Mkn 501 and Mkn 421 in the TeV range, in the case of Mkn 421 in both high and low states. In order to derive the time averaged spectrum of Mkn 501 (see also Section 2), which extends up to 17 TeV, we assume that despite the different levels of emission, the TeV  $\gamma$ -ray *spectrum* of Mkn 501 remains the same as that derived from the HEGRA data (Aharonian et al. 1999).<sup>1</sup> The

---

<sup>1</sup>CAT group claimed an evidence for spectral variability in Mkn 501  $\gamma$ -ray spectrum during the same observational period as HEGRA (Djannati-Atai et al. 1999). However CAT instrument has substantially lower energy threshold,  $E_{th} \simeq 250$  GeV, whereas HEGRA has energy threshold of about 500 GeV. Here we are interested in data around and above 1 TeV, where spectra taken at different fluxes have similar spectral shape.

same models are shown together with the X-ray data in Figs. 4 and 5. The complete SSC fits for Mkn 501 and Mkn 421 are shown in Figure 6 and 7.

Interestingly, the  $\gamma_{\max}$  values (see Table 1) providing the best fit to the data are very different for Mkn 421 and Mkn 501. The position of a peak in the de-absorbed  $\gamma$ -ray spectrum of Mkn 501 is at about 8 TeV, whereas for Mkn 421 it is at noticeably lower energy of about 2 TeV. The value of  $\gamma_{\max}$  strongly correlates with the maximum energy of the observed IC photons as given by e.g. Kino, Takahara & Kusunose (2002). We also find that the main difference between the high and low states of Mkn 421 can be accounted for by a change in  $\gamma_{\max}$  (as discussed earlier by (Fossati et al. 2000)) and in luminosity which, however, is not large.

Recent observations of Mkn 421 and Mkn 501, have revealed variability on the very short time scale of a few times  $\sim 10^3$ s (see Section 2). Combined with the fact that the de-absorbed spectrum of Mkn 501 is rather flat at TeV energies (Konopelko et al. 1999) (so that  $\nu_{c,27} > 1$ ), it is evident from Eq. (2) that the high Lorentz factors  $\sim 50$  are required to fit the observations, since this quantity is very insensitive to the other properties of the spectrum. This is in agreement with earlier estimates (Mastichiadis & Kirk 1997; Konopelko et al. 1999).

In order to check that the choice of the parameters does indeed lead to variations on the timescale  $t_{\text{var}}$  in the TeV regime, we performed time-dependent calculations. Starting from a stationary state, we impulsively changed the electron injection compactness by a factor of several and checked the behaviour of the flux at the TeV regime as it moved towards the new stationary state. We found that for all cases prescribed in Table 1, the e-folding time of the flux was always between  $t_{\text{var}}$  and  $2t_{\text{var}}$ .

Table 1. Summary of physical parameters used for the SSC models.

Source	State	$\delta$	$R$ (cm)	$s$	$\gamma_{\max}$	$l_e$	$B$ (G)	$t_{\text{cross}}/t_{\text{esc}}$	$\chi^2/\text{dof}$
Mkn 501	-	50	$1.5 \times 10^{15}$	1.55	$1.0 \times 10^6$	$6.20 \times 10^{-5}$	0.10	1.0	0.86
Mkn 421	high	55	$1.5 \times 10^{15}$	1.65	$3.0 \times 10^5$	$1.74 \times 10^{-5}$	0.45	1.0	0.33
Mkn 421	low	55	$1.5 \times 10^{15}$	1.65	$1.7 \times 10^5$	$1.15 \times 10^{-5}$	0.40	1.0	1.32

It is generally accepted that the X-ray fluxes from BL Lac objects like Mkn 421 and Mkn 501, are well correlated with the TeV  $\gamma$ -ray fluxes — the high state emission in X-rays appears at the same time in the TeV  $\gamma$ -rays. BL Lac objects can stay in a high emission state for more than 6 months (e.g., Mkn 501) and can at the same time be highly variable sources of both X-rays and  $\gamma$ -rays on a time scale of less than one hour. The spectral variations in TeV  $\gamma$ -rays are not well studied so far at such short time scales, even though there are clear indications for such variations (at least in case of Mkn 421, see Aharonian et al. (2002)).

The behavior of the X-ray emission of the BL Lac objects is sporadic, and also demonstrates very large flux variations on extremely short time scales of less than one hour (Sambruna et al. 2000; Catanese & Sambruna 2000). TeV  $\gamma$ -ray flares on similar time scales usually do not permit the accumulation of a sufficient number of  $\gamma$ -ray events with currently operating ground based Cherenkov detectors. Poor event statistics in such cases prevent the measurement of the energy spectrum well above 3 TeV, and make it difficult to detect the effects of IR absorption in such spectra. Thus, we feel it is premature to study in detail the correlations between the X-ray and multi-TeV  $\gamma$ -ray emission spectra on such short time scales, and have restricted our modelling to time-independent states.



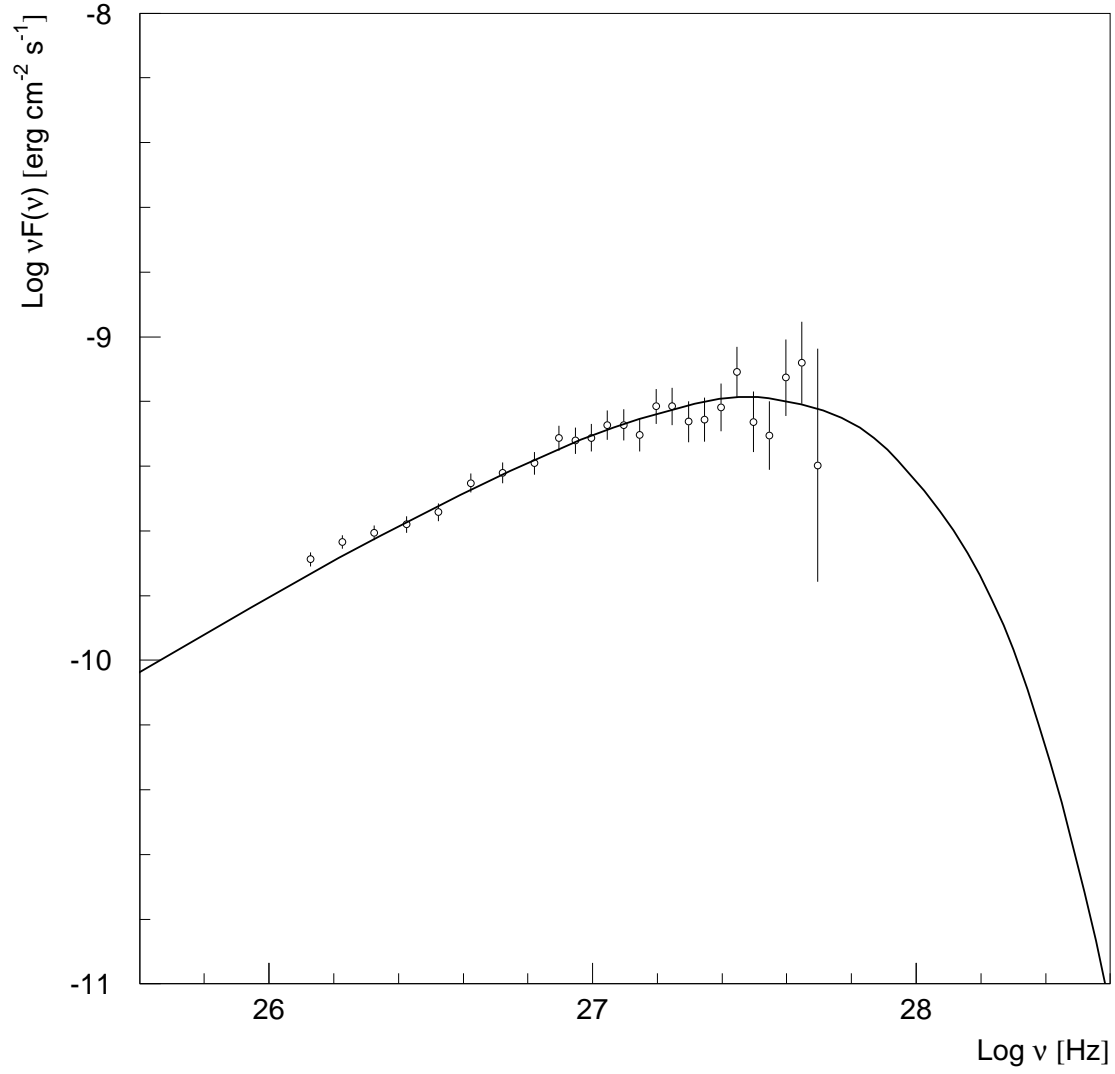


Fig. 2.— The de-absorbed spectrum of Mkn 501, with error bars indicating the uncertainty in intergalactic absorption, together with the best fit SSC model

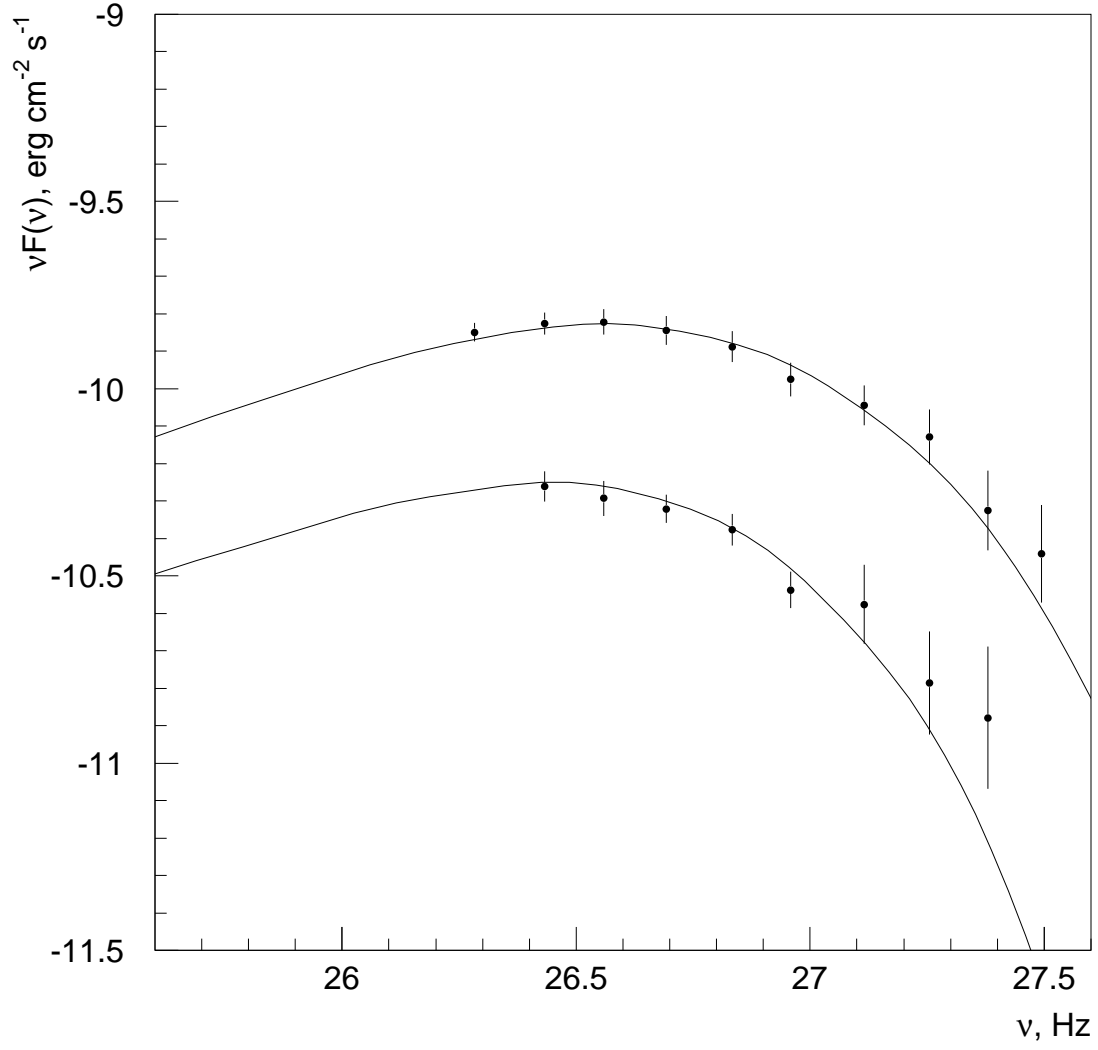


Fig. 3.— The de-absorbed spectrum of Mkn 421, with error bars indicating the uncertainty in intergalactic absorption, together with the best fit SSC models for both the high and low states

For Mkn 421 a variation of the spectral slope with flux level was recently discovered by HEGRA (Aharonian et al. 2002). However here we are not aiming to fit the X-ray and TeV  $\gamma$ -ray spectra for each particular flare, because the observational data in X-rays and TeV  $\gamma$ -rays are insufficient. Thus we consider here only two different spectra of X-ray and TeV  $\gamma$ -ray emission from Mkn 421 in lower and high state. It is important to mention that the position of the cut-off energy is the same in each case ( $E_0 = 3.6$  TeV).

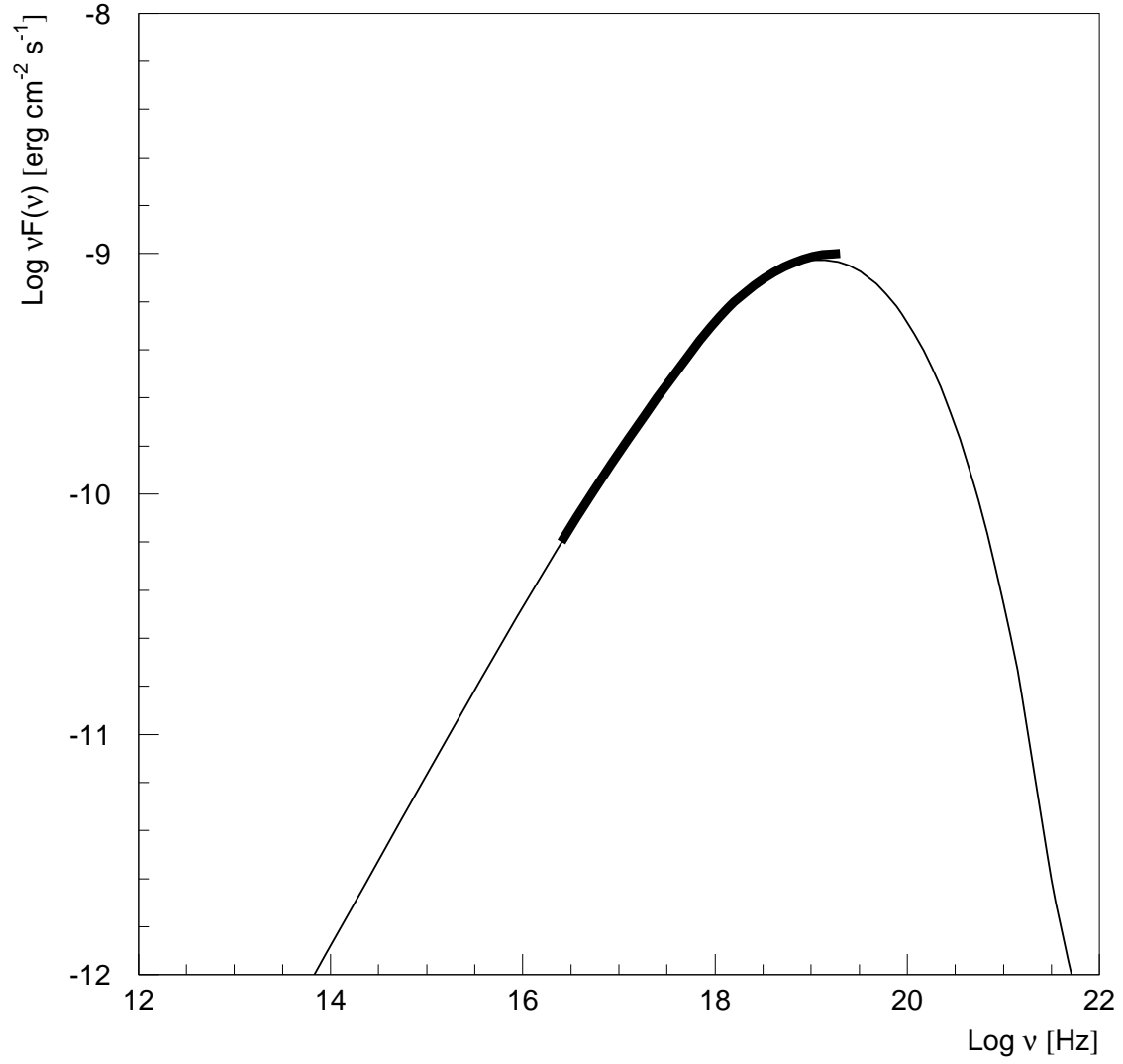


Fig. 4.— The X-ray spectrum of Mkn 501, together with the best fit SSC model

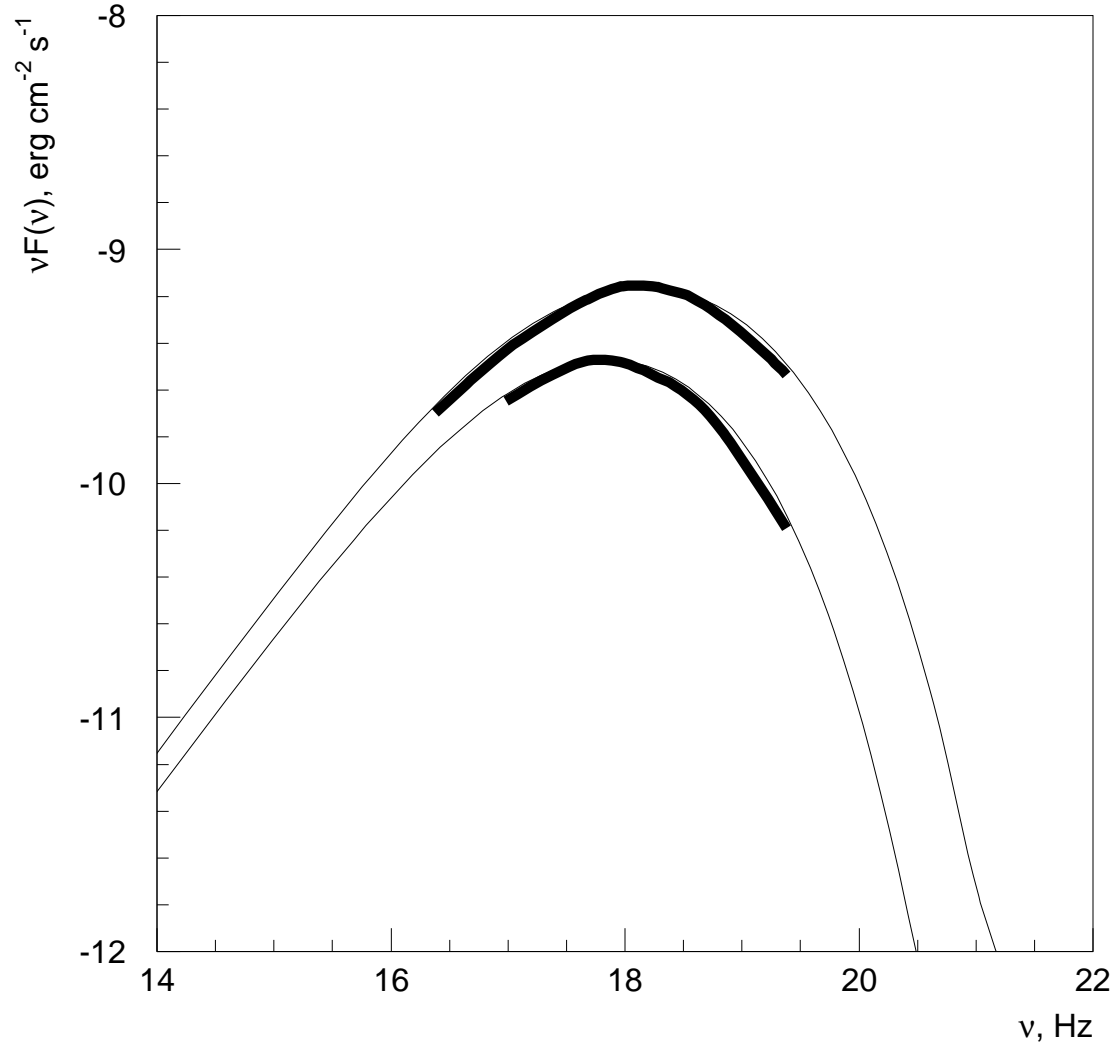


Fig. 5.— The X-ray spectrum of Mkn 421, together with the best fit SSC models for both the high and low states

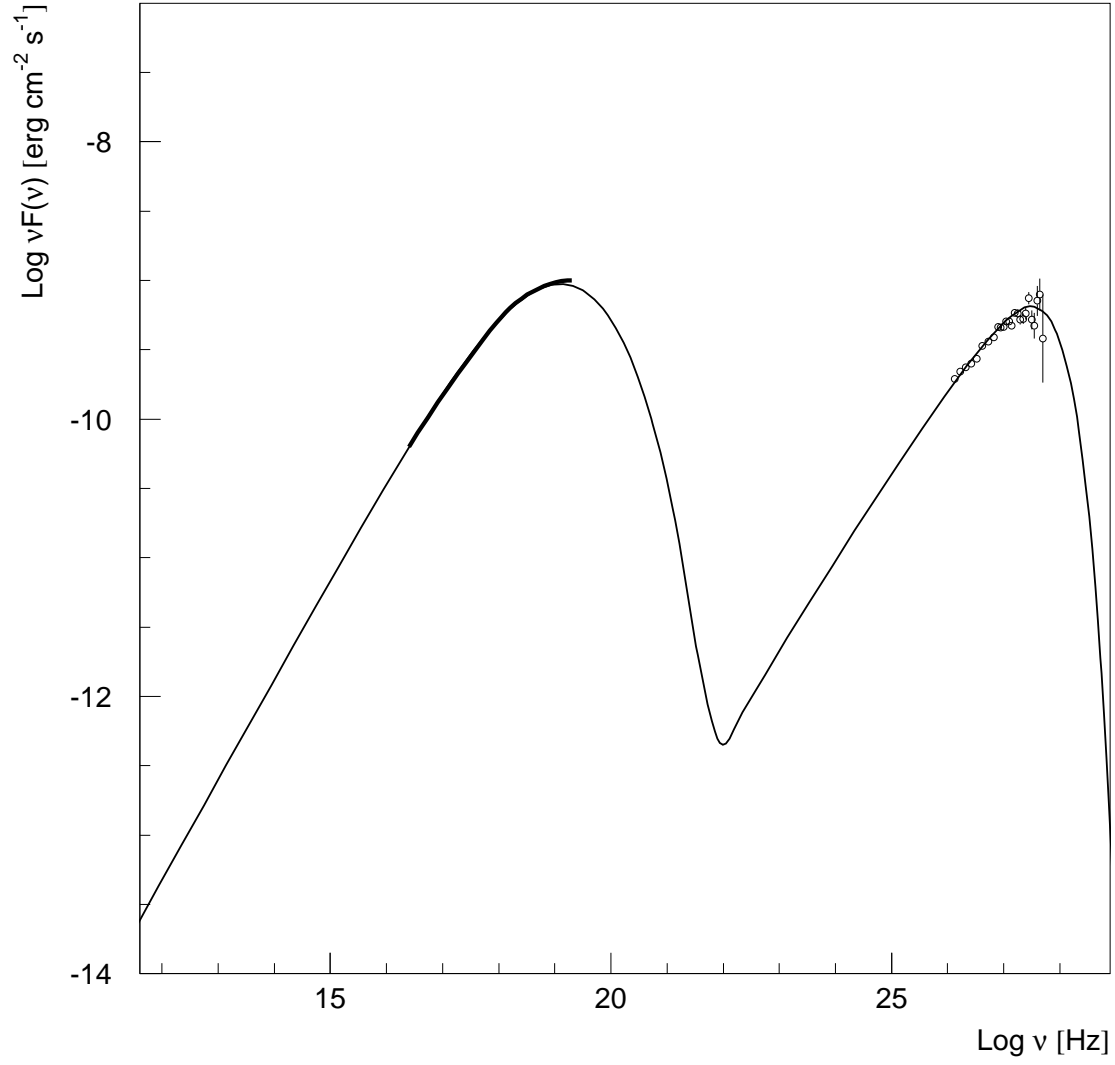


Fig. 6.— The combined X-ray/TeV  $\gamma$ -ray spectrum of Mkn 501 together with the best fit SSC model.

Figure 4 shows BeppoSAX measurements taken exactly during the 1997 outburst of Mkn 501. The X-ray and TeV  $\gamma$ -ray spectrum were averaged over different observing times but their fluxes at long time scales (month) are strongly correlated and finally X-ray to TeV  $\gamma$ -ray flux ratio remains almost unchanged.

## 5. Conclusion

We use here the data on the energy spectra of Mkn 501 and Mkn 421 over the energy range from 500 GeV up to  $\simeq 20$  TeV, which became available recently, to reconstruct the intrinsic, IR de-absorbed source spectra for both of these AGNs. Present uncertainties in EBL are treated here as the systematic errors of the de-absorbed spectra. We fit those intrinsic spectra of Mkn 501 and Mkn 421 (in low and high states) along with the X-ray data using the homogeneous SSC model.

Both the X-ray data and de-absorbed TeV  $\gamma$ -ray data can be fitted reasonably well by a homogeneous SSC model, even though the X-ray and TeV  $\gamma$ -ray features of both Mkn's are very different.

The two AGNs modelled have definitely different intrinsic spectra as well as slightly different variability scales. This leads to a slightly higher value of Doppler factor for Mkn 421 as well as a higher magnetic field and a lower value of  $\gamma_{\max}$ .

The energy spectra of Mkn 421 in high and low states can be fitted by changing the  $\gamma_{\max}$  and luminosity parameters, whereas the Doppler factor and the magnetic field remain unchanged.

In present analysis we used the X-ray and TeV  $\gamma$ -ray data, which are not simultaneous. They were averaged over not exactly the same but overlapping observing periods. This is because, first of all, one needs a substantially longer period to observe in TeV  $\gamma$ -rays and measure the spectrum over a broad multi-TeV region. Secondly, the shape of TeV  $\gamma$ -ray spectrum is more constraining than the absolute flux level. However, further dedicated multiwave campaigns for Mkn 421 and Mkn 501 may place a tighter limit on the choice of the model parameters.

We argue that a logically consistent SSC model of X-ray and TeV  $\gamma$ -ray emission can be constructed for both AGNs, Mkn 501 and Mkn 421, taking into account the IR absorption. Accurate spectral data are needed for other AGNs, in particular for the newly discovered 1ES 1426+428 and 1ES 1959+650, in order to test the consistency of this model for AGNs at different redshifts.

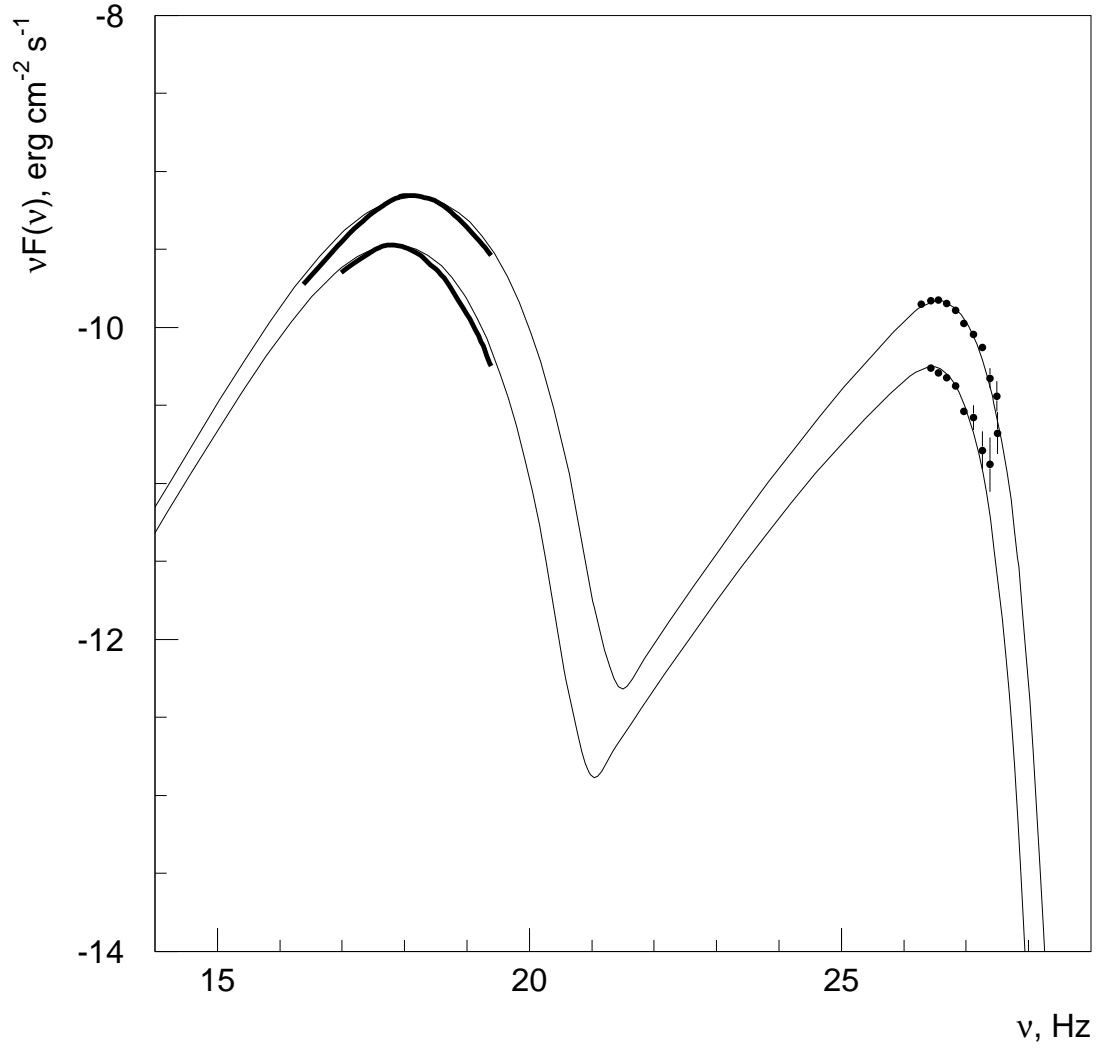


Fig. 7.— The combined X-ray/TeV  $\gamma$ -ray spectrum of Mkn 421, together with the best fit SSC models for both the high and low states.



## REFERENCES

- Aharonian, F., et al. 1999, *A&A*, 349, 11
- Aharonian, F., et al. 1999a, *A&A*, 350, 757
- Aharonian, F. 2000, *New Astronomy*, 5, 377
- Aharonian, F., et al. 2000, *ApJ*, 539, 317
- Aharonian, F., et al. 2001, *A&A*, 366, 62
- Aharonian, F., et al. 2001a, *ApJ*, 546, 898
- Aharonian, F., et al. 2002, submitted to *A&A*; astro-ph/0205499
- Aharonian, F., et al. 2002a, *A&A*, 384, 834
- Aharonian, F., et al. 2002b, *A&A*, 384, L23
- Barrau, A., et al. 1998, *NIM*, A416, 278
- Bradbury, S., et al. 1997, *A&A*, 320L, 5
- Catanese, M., et al. 1997, *ApJ*, 487, L143
- Catanese, M., et al. 1998, *ApJ*, 501, 616
- Catanese, M., Weekes, T.C. 1999, *The Publications of the Astronomical Society of the Pacific*, Volume 111, Issue 764, pp. 1193-1222.
- Catanese, M., Sambruna, R. 2000, *ApJ*, 534, L39
- Chadwick, P., et al. 1999, *ApJ*, 513, 161
- Costamante, L., et al. 2001, *A&A*, 371, 512
- de Jager, O.C., Stecker, F. 1998, *A&A*, 334L, 85
- de Jager, O.C., Stecker, F. 2002, *ApJ*, 566, 738
- Djannati-Atai, A., et al. 1999, *A&A*, 350, 17
- Djannati-Atai, A., 2002, submitted to *ApJ*, astro-ph/0207618
- Finkbeiner, D., Davis, M., Schlegel, D. 2000, *ApJ*, 544, 81

- Finley, J., et al. 2001, Proceedings of the 27th International Cosmic Ray Conference, ed. M. Simon, E. Lorentz & M. Pohl, (Hamburg, Germany: IUPAP), 7, 2827
- Fossati, G., et al. 2000, *ApJ*, 541, 153; 166
- Fossati, G., et al. April APS/HEAD Meeting, Albuquerque, Session B17 2002; Fossati, G., et al. 2002, in preparation.
- Franceschini, A., et al. 2001, *A&A*, 378, 1
- Gaidos, J., et al. 1996, *Nature*, 383, 319
- Gould, R., Schreder, G. 1966, *Phys. Rev. Letters*, 16, 252
- Hartman, R., et al. 1992, *ApJ*, 385, L1
- Hauser, M., Dwek, E. 2001, *ARA&A*, 39, 249
- Hofmann, W., et al. 2000 *Astropart. Phys.*, v. 12, iss. 4, 207
- Horan, D., et al. 2002, *ApJ*, 571, 753
- Horns, D., Konopelko, A. 2002, *IAU Circ.*, 7907, 2
- Inoue, S., Takahara, F. 1996, *ApJ*, 463, 555
- Kino, M., Takahara, F., Kusunose, M. 2002, *ApJ*, 564, 97
- Kneiske, T., Mannheim, K., Hartmann, D. 2002, *A&A*, 386, 1
- Konopelko, A., Kirk, J., Stecker, F., Mastichiadis, A. 1999, *ApJ*, 518, L13
- Konopelko, A., et al. 1999a, *Astropart. Phys.*, 10, 275
- Krawczynski, H., et al. 2001, *ApJ*, 559, 187
- Krawczynski, H., Coppi, P., Aharonian, F. 2002, submitted to *MNRAS*, astro-ph/0204229
- Krennrich, F., et al. 1999, *ApJ*, 511, 149
- Krennrich, F., et al. 2001, *ApJ*, 560, L45
- Krennrich, F., et al. 2002, submitted to *ApJ*, astro-ph/0207184
- Madau, P., Pozzetti, L. 2000, *MNRAS*, 312, L9
- Malkan, M., Stecker, F. 1998, *ApJ*, 496, 13

- Malkan, M., Stecker, F. 2001, ApJ, 555, 641
- Mannheim, K. 1993, A&A, 269, 67
- Mannheim, K. 1998, Science, Vol. 279, Iss. 5351, 684
- Mannheim, K., Biermann, P. 1992, A&A, 253L, 21
- Maraschi, L., Ghisellini, G., & Celotti, A. 1992, ApJ, 397L, 5
- Marscher, A., Travis, J. 1996, A&AS, 120, 537
- Mastichiadis, A., Kirk, J. 1995, A&A, 295, 613
- Mastichiadis, A., Kirk, J. 1997, A&A, 320, 19
- Mohanty, G., et al. 1998, Astropart. Phys., Vol. 9, Issue 1, 15
- Mücke, A., Protheroe, R. 2001, Astroparticle Phys., 15, 121
- Nikishov, A., 1962, Sov. Phys. JETP, 14, 393
- Nishiyama, T., et al. 2000, AIP Conf. Proc. 516, Proceedings of the 26th International Cosmic Ray Conference, ed. B.L. Dingus, D.B. Kieda & M.H. Salamon (Salt Lake City, Utah:AIP), 3, 370
- Ong, 1998, Physics Reports, 305, 93-202
- Petry, D., et al. 1996, A&A, 311, L13
- Petry, D., et al. 2000, ApJ, 536, 742
- Petry, D., et al. 2002, submitted to ApJ, astro-ph/0207506
- Pian, E., et al. 1997, ApJ, 486, 784
- Primack, J., 2002, astro-ph/0201119
- Protheroe, R., Meyer, H. 2000, Phys. Lett. B493, 1
- Punch, M., et al. 1992, Nature, 358, 477
- Quinn, J., et al. 1996, ApJ, 456, L83
- Renault, C., et al. 2001, A&A, 371, 771
- Remillard, R., et al. 1989, ApJ, 345, 140

- Rowan-Robinson, M. 2001, *ApJ*, 549,745
- Sambruna, R., et al. 2000, *ApJ*, 538, 127
- Samuelson, F., et al. 1998, *ApJ*, 501, L17
- Stecker, F., de Jager, O.C., Salamon, M. 1992, *ApJ*, 390, L49
- Tan, J.C., Silk, J., & Balland, C. 1999, *ApJ*, 522, 579
- Tavecchio, F., Maraschi, L., & Ghisellini, G. 1998, *ApJ*, 509, 608
- Tavecchio, F., et al. 2001, *ApJ*, 554, 725
- Thompson, D., et al. 1995, *ApJS*, 101, 259
- Weekes, T., et al. 2002, *IAU Circ.*, 7903, 1
- Xu, C., 2000, *ApJ*, 541, 134